Supporting information for

Doping trace cerium in ZSM-48 in situ during hydrothermal synthesis for efficient hydroisomerization of long-chain n-alkane

Wenjun Zhang [a], MingWei Zhang, Linlin Liu, Songzu Tang, Li Wang Xiangwen Zhang [a,b] and Guozhu Li [a,b] *

[a] Key Laboratory for Green Chemical Technology of Ministry of Education, School of Chemical Engineering and Technology, Tianjin University, Tianjin 300072, China

[b] Collaborative Innovation Center of Chemical Science and Engineering (Tianjin), Tianjin 300072, China

*Corresponding author. Tel./fax: +86 22 27892340.

E-mail address: gzli@tju.edu.cn

Calculation of correlation coefficient.

Firstly, the properties and catalytic performance of different catalysts was summarized to obtain an initial matrix. Afterwards, the Spearman correlation coefficient calculation formula was used to calculate the correlation coefficient (ρ) between each property characteristic and catalytic performance as listed below.

$$\rho = \frac{\sum_i (x_i - \bar{x})(y_i - \bar{y})}{\sqrt{\sum_i (x_i - \bar{x})^2 \sum_i (y_i - \bar{y})^2}}$$

Finally, the as-calculated correlation coefficients were summarized and plotted.

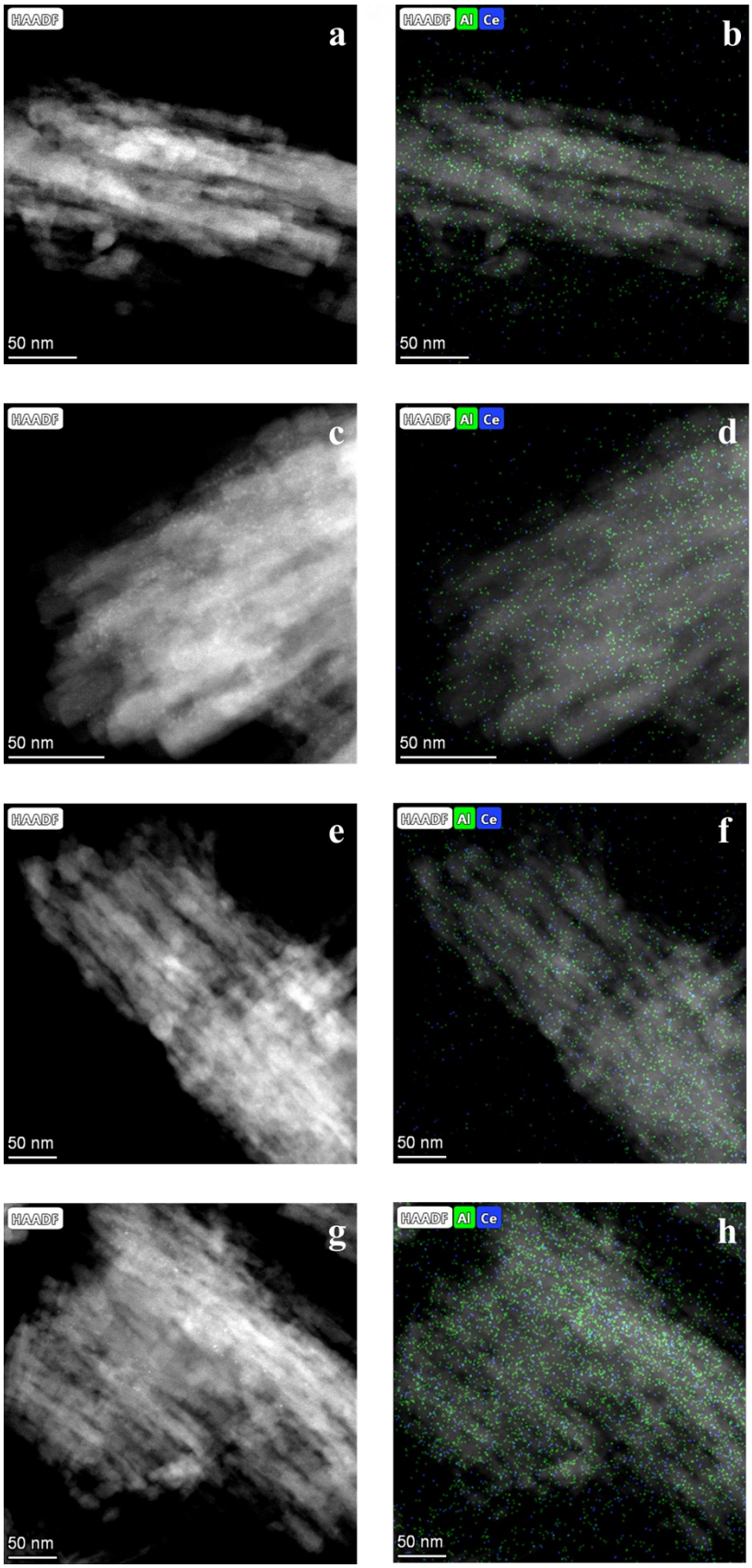

Figure S1 HRTEM-STEM and EDS images of (a-b) ZSM-48-9, (c-d) ZSM-48-7, (e-f) ZSM-48-5 and (g-h) ZSM-48-3.

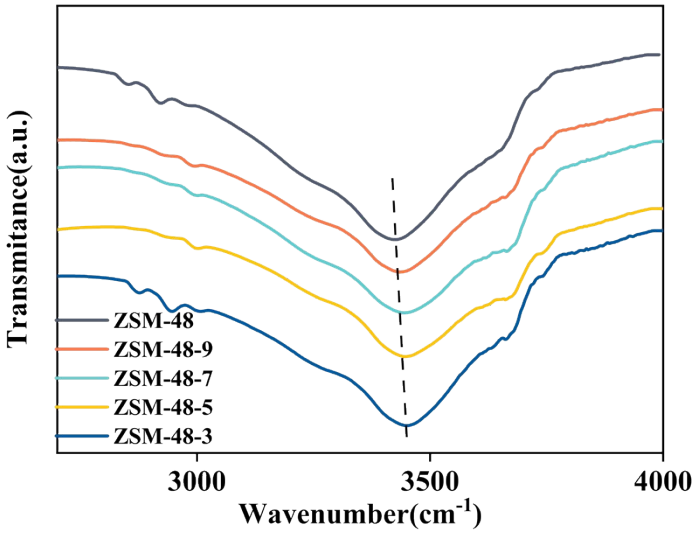

Figure S2 FT-IR of spectra of different samples in the $\nu_{(OH)}$ region.

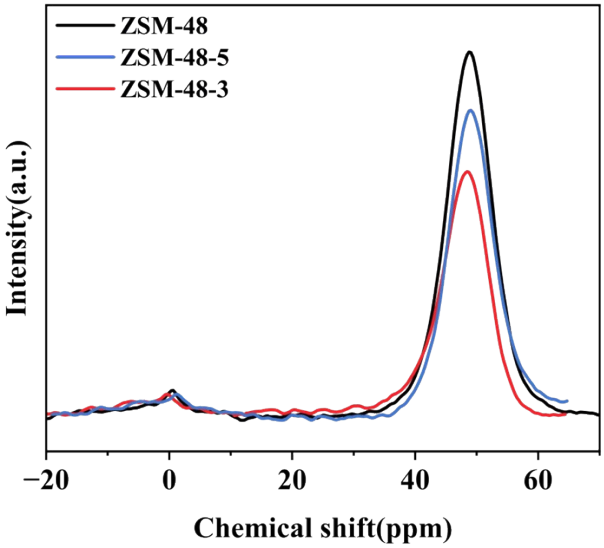

Figure S3 ^{27}Al MAS NMR spectra of ZSM-48, ZSM-48-5 and ZSM-48-3.

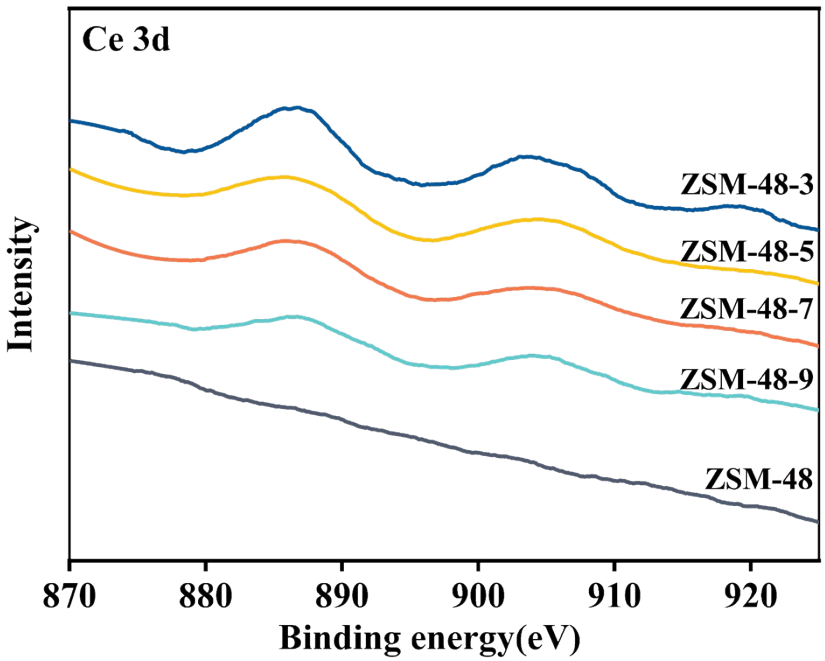

Figure S4 XPS spectra of Ce 3d for ZSM-48 and ZSM-48-x samples.

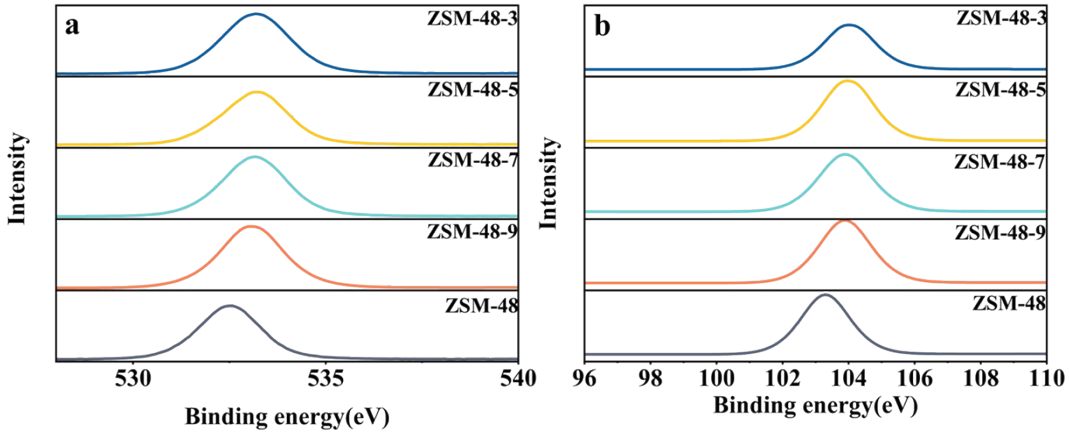

Figure S5 XPS spectra of (a) O 1s and (b) Si 2p for ZSM-48 and ZSM-48-x samples.

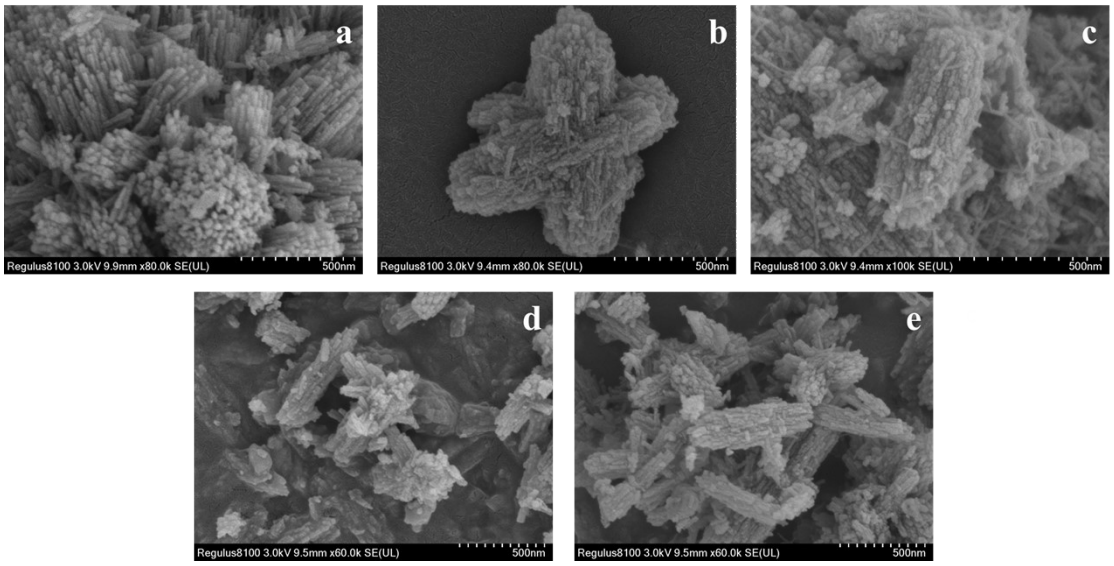

Figure S6 SEM images of (a) ZSM-48, (b) ZSM-48-9, (c) ZSM-48-7, (d) ZSM-48-5, (e) ZSM-48-3.

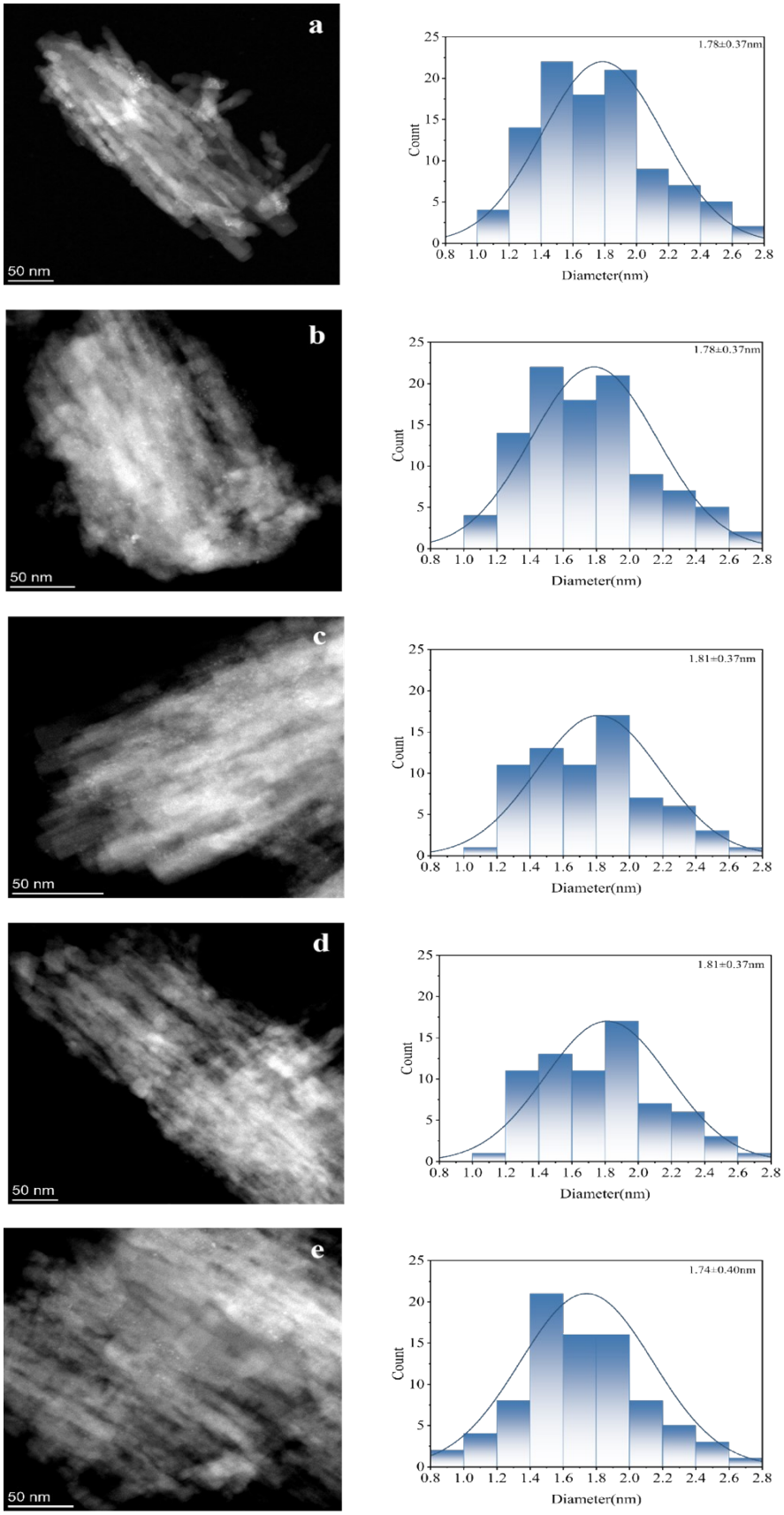

Figure S7 HAADF-STEM images of Pt nanoparticles and particle size distribution in (a) Pt/ZSM-48, (b) Pt/ZSM-48-9, (c) Pt/ZSM-48-7, (d) Pt/ZSM-48-5, and (e) Pt/ZSM-48-3.

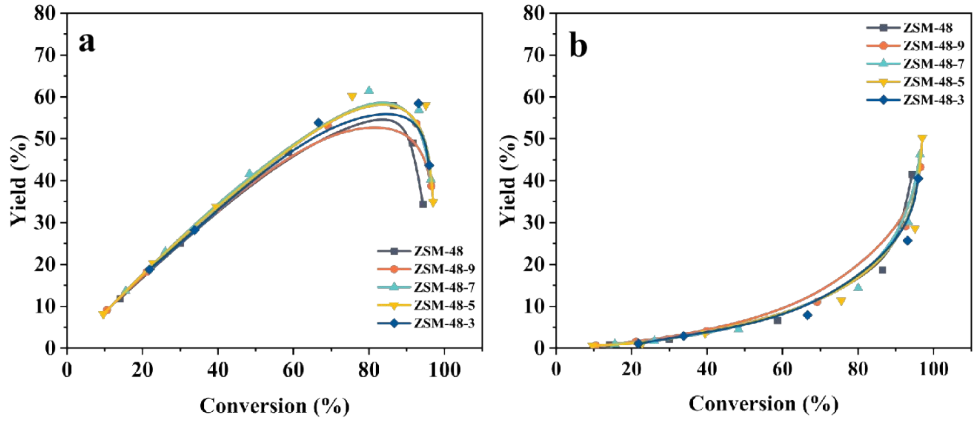

Figure S8 Distribution of the yields of (a) mono-branched isomers and (b) multi-branched isomers on Pt/ZSM-48 and Pt/ZSM-48-x.

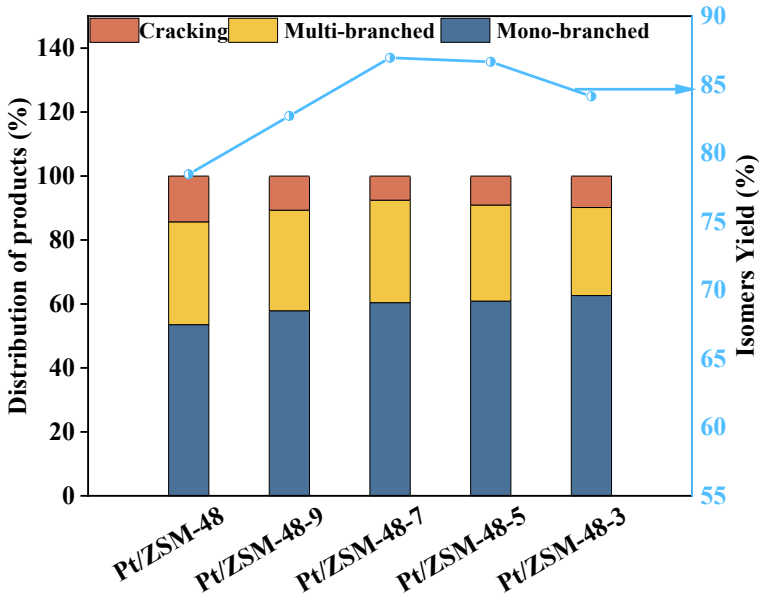

Figure S9 The maximum isomer yields of i-C_{16}, and the distribution of products (mono-branched, multi-branched and cracking) on Pt/ZSM-48 and Pt/ZSM-48-x.

Table S1 The isomer (*i*-C_{16}) yield on different catalysts reported in literature.

Catalysts	Isomer yield (%)	Mono yield (%)	Multi yield (%)	Temperature (°C)	Literature
Pt/ZSM-48-0.02	81.0	49.4	31.6	310	[1]
Pt/ZSM-48(H)	86.0	38.7	47.3	330	[2]
Pt/Z(H)80	80.0	48.0	32.0	-	[3]
Pt/A-48	81.0	63.0	18.0	310	[4]
Pt/ZSM-48-DA-2	89.0	59.5	29.5	310	[5]

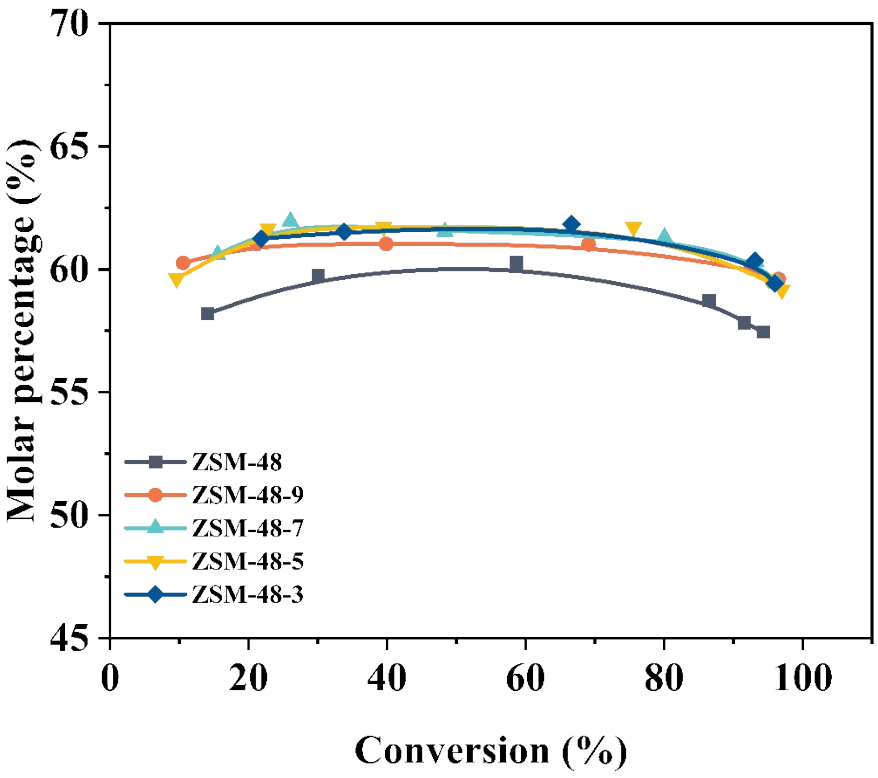

Figure S10 Molar proportions of 5-/6-/7-/8-methylpentadecane in the mono-methyl isomers on different catalysts.

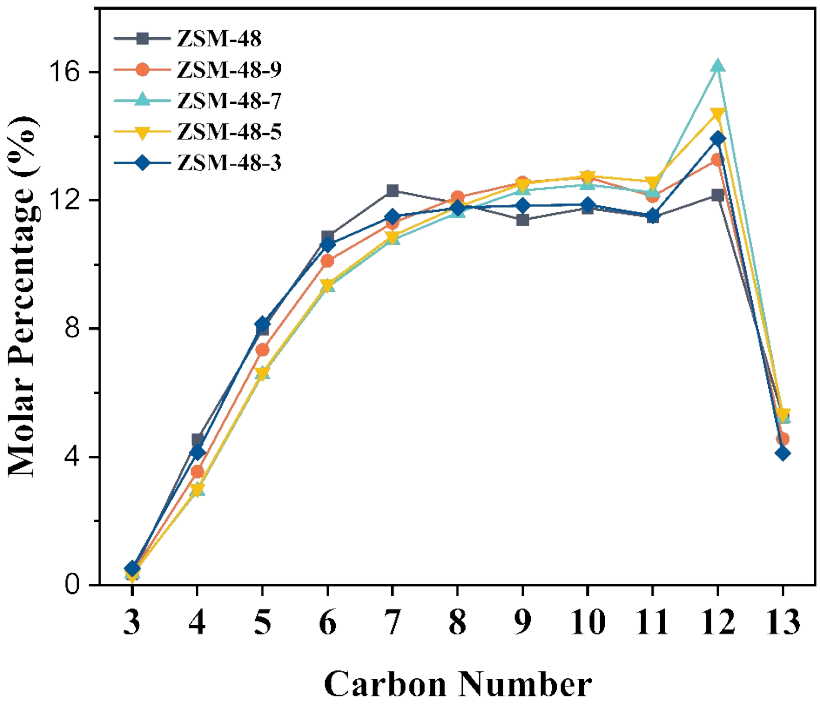

Figure S11 The carbon number distribution of the cracking products.

References

[1] C. Zou, J. Meng, J. Zhao, J. Liu, C. Li, X. Chen, C. Liang, *Mole. Catal.* **2024**, 561,114160.

[2] J. Meng, T. Cui, D. Bai, C. Li, X. Chen, C. Liang, *Fuel* **2022**, 324, 124589.

[3] J. Meng, D. Bai, P. Zeyaodong, C. Li, X. Chen, C. Liang, *Microporous Mesoporous Mat.* **2022**, 330, 111637.

[4] W. Zhao, L. Liu, X. Niu, X. Yang, J. Sun, Q. Wang, *Fuel* **2023**, 349, 128703.

[5] M. Zhang, L. Liu, W. Zhang, X. Zhang, G. Li, *Microporous Mesoporous Mat.* **2023**, 356, 112597.